Preferential oligomerization of isobutene in a mixture of isobutene and 1-butene over sodium-modified 12-tungstosilicic acid supported on silica

Jin Zhang[a], Mitsuru Kanno[a], Jiao Zhang[a], Ryuichiro Ohnishi[b], Kakeru Toriyabe[c]

Hiromi Matsuhashi[c], Yuichi Kamiya[b]*

[a]*Graduate School of Environmental Science, Hokkaido University, Sapporo 060-0810, Japan*

[b]*Research Faculty of Environmental Earth Science, Hokkaido University, Sapporo 060-0810, Japan*

[c]*Department of Science, Hokkaido University of Education, 1-2 Hachiman-cho, Hakodate 040-8567, Japan*

*Corresponding author:

Yuichi Kamiya

Tel: +81-11-706-2217

Fax: +81-11-706-2217

E-mail: kamiya@ees.hokudai.ac.jp

ABSTRACT

Modification of 15 wt% $H_4SiW_{12}O_{40}/SiO_2$ with Na^+ ions was investigated. Na-modified $H_4SiW_{12}O_{40}/SiO_2$ showed higher selectivity for isobutene oligomerization in the preferential oligomerization of isobutene in an equimolar mixture of isobutene and 1-butene than the unmodified one and the selectivity increased with an increase in the Na^+ ion content. The highest selectivity (~97%) was achieved by using $Na_3HSiW_{12}O_{40}/SiO_2$. The activity decreased with an increase in the Na^+ ion content. Unmodified $H_4SiW_{12}O_{40}/SiO_2$ had two kinds of acid sites with different acid strengths (medium and strong acid sites) on the outermost surface as revealed by temperature-programmed desorption of benzonitrile. However, the strong acid sites were eliminated by modification with alkaline metal cations; for example, $Na_3HSiW_{12}O_{40}/SiO_2$ had a negligible amount of strong acid sites. Thus, we concluded that the absence of strong acid sites on the outermost surface is the reason for the high selectivity. $Li_3HSiW_{12}O_{40}/SiO_2$ and $K_3HSiW_{12}O_{40}/SiO_2$ also exhibited high selectivity for isobutene oligomerization with activities comparable to that of $Na_3HSiW_{12}O_{40}/SiO_2$.

Keywords: supported heteropolyacid; modification with alkali metal cations; isobutene oligomerization; surface acidity; temperature-programmed desorption

1. Introduction

C4 hydrocarbons, including linear butenes (1-butene, *cis*-2-butene, and *trans*-2-butene) and isobutene, are important raw materials for various chemicals, such as 2-butanol, methyl ethyl ketone, methyl methacrylate, and polymers. In order to utilize C4 hydrocarbons, one must separate isobutene as well as butadiene from mixtures, which are produced from fluid catalytic cracking (FCC) of heavy oil and steam cracking of naphtha in petroleum refineries and petrochemical factories. However, the separation of isobutene from butene isomers is difficult because they have similar boiling points. One potential method for the separation of isobutene from mixtures of butenes involves the preferential oligomerization of isobutene (meaning that isobutene rather than linear butenes reacts selectively in a mixture of butenes) over solid acid catalysts. Although preferential oligomerization of isobutene over SiO_2-Al_2O_3 catalysts has been commercialized, loss of linear butenes due to low selectivity remains a serious problem [1]. In our previous work [2], we have investigated the preferential oligomerization of isobutene in an equimolar mixture of isobutene and 1-butene over $H_4SiW_{12}O_{40}/SiO_2$ with various $H_4SiW_{12}O_{40}$ loadings (10–60 wt%) and have found that low loading catalysts such as 10 wt% $H_4SiW_{12}O_{40}/SiO_2$ shows high selectivity for the isobutene oligomerization as well as high activity. However, a further increase in the selectivity is needed to reduce the loss of linear butenes.

Since the amount, strength, and type of acid sites are crucial factors controlling catalytic performance, including activity, selectivity, and life, of solid acids [3,4]. Among them, acid strength has the most significant influence on the catalytic performance. One method for controlling the acidic properties of solid acids is to modify them with alkaline metal cations or alkaline earth metal cations. O'Donoghue and Barthomeuf [5] have reported that the activity for dehydration of 2-propanol over alkaline metal cation-substituted Y-type zeolites with high cation contents decreased as follows: Li-H-Y > Na-H-Y >> Rb-H-Y. This order agrees with the acid strength of the Brønsted OH groups determined on the basis of the wavenumber of the OH stretch in the IR spectra. Xu et al. [6] have reported that the activity for the aldol condensation of acetone decreases in the order of H-ZSM-5 > H-Y > H-X > Na-H-X, Cs-H-X > Cs-H-Y, Cs-H-ZSM-5. This order is in good agreement with the strength of the Brønsted acid determined from the chemical shift in ^{13}C MAS NMR spectra of the mesityl oxide adsorbed on the acids. Cañizares and Carrero [7] have investigated the modification of a ferrierite zeolite with alkaline earth metal cations, including Mg^{2+}, Sr^{2+}, and Ba^{2+}, and have found that the acid strength becomes weaker in the following order: $H^{+} > Mg^{2+} > Sr^{2+} > Ba^{2+}$. Niwa and his coworkers have found by using a technique combining TPD and IR spectra of ammonia, referred to as an ammonia IRMS-TPD technique, that the acid strength of the Brønsted OH group located in the supercage of a Y-type zeolite is enhanced by ion-exchange with Ca^{2+} and

Ba^{2+} [8]. This finding has further been supported via periodic DFT calculations [9].

In the present study, we investigated the effects of modifying $H_4SiW_{12}O_{40}/SiO_2$ with sodium cation on the catalyst performance for the preferential oligomerization of isobutene in an equimolar mixture of isobutene and 1-butene. The Na^+ ion content in the Na-modified $H_4SiW_{12}O_{40}/SiO_2$ was systematically changed, and the effects on the catalytic performance and acidic properties were investigated. The acidic properties were assessed by using temperature-programmed desorptions of ammonia (NH_3-TPD) and benzonitrile (BN-TPD), and from heat of argon adsorption on the catalysts. The BN-TPD can be used to determine the amount and acid strength of the acid sites located on the outermost surface of $H_4SiW_{12}O_{40}/SiO_2$ [10-12]. Modification of $H_4SiW_{12}O_{40}/SiO_2$ with Li^+ and K^+ were also investigated.

2. Experimental

2.1 Catalysts

The heteropolyacid $H_4SiW_{12}O_{40}$ (Nippon Inorganic Color Chemical Co.) was supported on SiO_2 (Aerosil 300, 274 $m^2\ g^{-1}$) by using an incipient wetness method, as described in Ref. [2]. An aqueous solution of $H_4SiW_{12}O_{40}$ (0.08 mol dm^{-3}) was added dropwise onto the SiO_2 at room temperature to form a wet solid. The wet solid was dried in an oven at 333 K overnight and then calcined at 523 K in air for 5 h. The loading amount of $H_4SiW_{12}O_{40}$ was adjusted to 15

wt%.

Na-modified $H_4SiW_{12}O_{40}/SiO_2$ was prepared in a similar manner to $H_4SiW_{12}O_{40}/SiO_2$. An aqueous solution of $H_4SiW_{12}O_{40}$ and Na_2CO_3 (Wako Pure Chem. Ind. Ltd) was used instead of an aqueous solution of $H_4SiW_{12}O_{40}$. The samples $Na_xH_{4-x}SiW_{12}O_{40}/SiO_2$, where x = 1, 2, 3, and 4, were prepared by changing the concentration of Na_2CO_3. $Li_3HSiW_{12}O_{40}/SiO_2$ and $K_3HSiW_{12}O_{40}/SiO_2$ were also prepared in a similar manner to $Na_3HSiW_{12}O_{40}/SiO_2$, although Li_2CO_3 (Wako Pure Chem. Ind. Ltd) and K_2CO_3 (Wako Pure Chem. Ind. Ltd), respectively, were used instead of Na_2CO_3.

2.2 Preferential oligomerization of isobutene in a mixture of 1-butene and isobutene over $Na_xH_{4-x}SiW_{12}O_{40}/SiO_2$

Preferential oligomerization of isobutene in a mixture of 1-butene and isobutene (mole ratio of 1-butene:isobutene = 1:1, Takachiho Chemical Ind. Co., Ltd.) was performed in a stainless steel autoclave (Taiatsu Techno Co., 30 cm^3) at 293 K in a similar manner to that described in Ref. [2]. The reaction was also conducted at 333 K. A mixture of hexane (1.5 cm^3, Kanto Chemical Co.) and dodecane (0.15 cm^3, 0.1 g, Kanto Chemical Co.), which were used as the solvent and internal standard, respectively, and 0.1 g of the catalyst were introduced into the reactor. Then, a mixture of isobutene and 1-butene (8 cm^3, 4.8 g) was introduced into

the reactor by using a pressure resistant syringe, followed by the introduction of hexane (2.5 cm^3) using the same syringe in order to rinse it. After purging with N_2 five times to remove the air inside the reactor, the temperature was decreased to 293 K or increased to 333 K with vigorous stirring (300 rpm) using a magnetic stirrer. All pipe fittings on the reactor were heated to about 353 K.

The products in the gas phase were analyzed by using a gas chromatograph (Shimadzu, GC-14B) equipped with a capillary column (CP-Al_2O_3/KCl PLOT, 25 m × 0.25 mm, Varian, Inc.) and a flame ionization detector (FID-GC). Liquid samples of the products were analyzed by using an FID-GC (Shimadzu, GC-14A) equipped with a capillary column (Rtx-1 PONA, 30 m × 0.32 mm, Restec Co.).

The conversion and selectivity for isobutene oligomerization were defined as:

$$\text{Conversion of isobutene (\%)} = \frac{\text{mol of isobutene consumed}}{\text{mol of initial isobutene}} \times 100$$

$$\text{Conversion of linear butene (\%)} = \frac{\text{mol of linear butene consumed}}{\text{mol of initial 1-butene}} \times 100$$

$$\text{Selectivity for isobutene oligomerization (\%)} = \frac{\text{conversion of isobutene}}{\text{conversion of isobutene + conversion of linear butene}} \times 100$$

In order to simplify the calculation, 1-butene and 2-butenes (*cis*-2-butene and *trans*-2-

butene) were combined and called linear butenes, although only 1-butene was used as a reactant.

2.3 Characterization

X-ray diffraction (XRD) patterns were measured on an XRD diffractometer (Miniflex, Rigaku) with Cu Kα radiation (λ = 0.154 nm). IR spectra of the catalysts were recorded on an IR spectrometer (FT-IR/230, JASCO) using a catalyst pellet diluted with KBr. Specific surface areas were estimated by using the Brunauer–Emmett–Teller (BET) equation with an adsorption isotherm of N_2 at 77 K, which was measured on a Belsorp-mini instrument (BEL Japan Inc.).

Temperature-programmed desorption of ammonia (NH_3-TPD) was carried out by using a multi-task TPD system (BEL Japan Inc.) equipped with a quadrupole mass spectrometer (Anelva; M-QA100S). After pretreatment at 523 K for 2 h in a flow of He (50 cm^3 min^{-1}), the catalyst was exposed to NH_3 at 13 kPa and 373 K for 0.5 h, and then the excess NH_3 was removed in a He flow at 373 K for 0.5 h. The temperature of the sample was increased at a rate of 10 K min^{-1} to 973 K, and the desorbed gas was monitored at m/z = 16.

Benzonitrile-TPD profiles were obtained by using a homemade TPD system equipped with a flame ionization detector. After pretreatment at 523 K in a flow of N_2 (40 cm^3 min^{-1}), the catalyst was exposed to 0.122 μmol h^{-1} of benzonitrile at 373 K for 1 h. The weakly adsorbed or physisorbed benzonitrile was removed in an N_2 flow by heating to 373 K and then to 393 K.

The temperature was increased at a rate of 10 K min^{-1} to 973 K, while the FID signal of the exit gas was monitored.

Adsorption isotherms of Ar at 203–233 K were taken on an automatic adsorption apparatus (BEL Japan Inc.). Calculation of the adsorption heat of Ar was done according to the method reported in Ref. [13]

3. Results

3.1 Preferential oligomerization of isobutene in a mixture of butenes over $Na_xH_{4-x}SiW_{12}O_{40}/SiO_2$

Fig. 1 shows time courses for the conversion of isobutene and linear butenes at 293 K over $Na_xH_{4-x}SiW_{12}O_{40}/SiO_2$ with different Na^+ ion contents (x = 0–3). Since $Na_4SiW_{12}O_{40}/SiO_2$ (x = 4) was inactive for the reaction due to the absence of acid sites, it was not included in Fig. 1. The conversions of both isobutene and linear butenes increased with the reaction time; however, those of linear butenes were significantly lower than those of isobutene, regardless of the reaction time and the Na^+ ion content; conversions of isobutene and linear butenes over $H_4SiW_{12}O_{40}/SiO_2$ (x = 0) at 3 h were 42.1 and 3.2%, respectively. It is noted that the conversion of linear butenes over $Na_3HSiW_{12}O_{40}/SiO_2$ (x = 3) at 24 h was only 0.8%, while that of isobutene was 41.0%.

We assumed that both oligomerizations of isobutene and linear butenes were a first-order

reaction and estimated the first-order reaction rate constants for each reaction, which are denoted by *k*(*iso*-) and *k*(*n*-), respectively, by fitting them to the experimental data shown in Fig. 1. In Fig. 2, *k*(*iso*-) and *k*(*n*-) as well as the ratios of *k*(*iso*-)/*k*(*n*-) are plotted as a function of the Na^+ ion content. While both *k*(*iso*-) and *k*(*n*-) decreased with an increase in the Na^+ ion content, *k*(*n*-) dropped down more remarkably than *k*(*iso*-). In fact, the *k*(*iso*-)/*k*(*n*-) ratio was 16.4 for $H_4SiW_{12}O_{40}/SiO_2$, and that for $Na_3HSiW_{12}O_{40}/SiO_2$ was much larger, being 62.9.

In Fig. 3, the selectivity for isobutene oligomerization is plotted against the conversion of isobutene. The selectivity for isobutene oligomerization was defined as the isobutene conversion divided by total conversion, which is a sum of isobutene conversion and linear butenes conversion, and multiplied by 100 (see Experimental). The selectivities were basically independent of the isobutene conversions. $H_4SiW_{12}O_{40}/SiO_2$ showed the selectivity of 92%. The selectivity increased with an increase in the Na^+ ion content and reached a maximum (about 97%) for $Na_3HSiW_{12}O_{40}/SiO_2$. These results demonstrated that the modification of $H_4SiW_{12}O_{40}/SiO_2$ with Na^+ ion is an effective method for improving the selectivity for the preferential oligomerization of isobutene.

3.2 Physical properties of $Na_xH_{4-x}SiW_{12}O_{40}/SiO_2$

Fig. 4 shows XRD patterns and IR spectra of $Na_xH_{4-x}SiW_{12}O_{40}/SiO_2$ (x = 0, 1, 2, and 3) and

the SiO_2 support. Regardless of the Na^+ ion content, no diffraction lines were observed in the XRD patterns (Fig. 4A), indicating that heteropoly anions were highly dispersed on the SiO_2. In the IR spectra (Fig. 4B), characteristic bands due to the Keggin structure (ν_{as}(W=O) = 980 cm^{-1}, ν_{as}(Si-O) = 926 cm^{-1}, and ν_{as}(W-O-W) = 878 cm^{-1}) were observed for each $Na_xH_{4-x}SiW_{12}O_{40}/SiO_2$, indicating that the Keggin structure was basically intact.

The specific surface areas of $Na_xH_{4-x}SiW_{12}O_{40}/SiO_2$ were 207, 195, 194, and 204 $m^2\ g^{-1}$ for x = 0, 1, 2, and 3, respectively. If $H_4SiW_{12}O_{40}$ is highly dispersed on SiO_2, the surface area of $H_4SiW_{12}O_{40}/SiO_2$ should be 233 $m^2\ g^{-1}$ or less because the surface area of SiO_2 was 274 $m^2\ g^{-1}$ (274 × 0.85 = 233 $m^2\ g^{-1}$). This is nearly the same as the surface area (207 $m^2\ g^{-1}$) of $H_4SiW_{12}O_{40}/SiO_2$. For the Na-modified catalysts, regardless of the Na^+ ion content, the surface area was about 200 $m^2\ g^{-1}$. Thus, we do not think that a porous Na salt of $H_4SiW_{12}O_{40}$ forms on SiO_2.

3.3 Acidic properties of $Na_xH_{4-x}SiW_{12}O_{40}/SiO_2$

Fig. 5 shows NH_3-TPD profiles for $Na_xH_{4-x}SiW_{12}O_{40}/SiO_2$ (x = 0, 1, 2, and 3). Since NH_3 was not only adsorbed on the surface of solid heteropolyacids but also absorbed into their bulk, NH_3-TPD profile exhibits the acidic properties of bulk of the heteropolyacids [14]. The NH_3-TPD profile for $H_4SiW_{12}O_{40}/SiO_2$ (Fig. 5a) was broad and consisted of poorly separated three

peaks near 550 (shoulder), 660, and 750 K (shoulder), which are labeled as W_{bulk} acid sites, MS_{bulk} acid sites, and S_{bulk} acid sites, respectively. Although the peak positions of MS_{bulk} acid sites were shifted toward lower temperature with an increase in the Na^+ ion content, these are probably due to an decrease in the acid sites present in the TPD cell, as demonstrated by Niwa et al. [15].

The amounts of total acid sites estimated by using NH_3-TPD are plotted as a function of the Na^+ ion content in Fig. 6A, in which the broken line represents the total amount of protons present in $Na_xH_{4-x}SiW_{12}O_{40}/SiO_2$ calculated from the chemical formula ($Na_xH_{4-x}SiW_{12}O_{40}$) and the loading amount (15 wt%). The amounts of total acid sites decreased monotonically with an increase in the Na^+ ion content, and were about the same as the calculated number of protons in $Na_xH_{4-x}SiW_{12}O_{40}/SiO_2$, although the acid amount of unmodified $H_4SiW_{12}O_{40}/SiO_2$ was slightly larger than that of the calculated value. This correlation clearly indicates that $H_4SiW_{12}O_{40}$ is neutralized with Na^+ ions; i.e., Na^+ ions were stoichiometrically substituted for protons of $H_4SiW_{12}O_{40}$.

The spectrum of NH_3-TPD was deconvoluted by using a peak-fitting program, Fityk, provided that the spectrum was composed of three peaks with Gaussian function. The peak areas of each acid site are plotted in Fig. 6B. The MS_{bulk} acid sites accounted for the majority of the acid sites and its amount decreased monotonically with an increase in the Na^+ ion content.

On the other hand, the amount of W_{bulk} acid sites slightly changed from x = 0 to 1 and then decreased as the Na^+ ion content further increased. The amounts of S_{bulk} acid sites were nearly constant irrespective of the Na^+ ion content.

Fig. 7 shows benzonitrile -TPD profiles for $Na_xH_{4-x}SiW_{12}O_{40}/SiO_2$. The benzonitrile-TPD profiles were remarkably different from the NH_3-TPD ones. Three distinct peaks were observed at approximately 470, 620, and 730 K in the benzonitrile-TPD profile for $H_4SiW_{12}O_{40}/SiO_2$ (Fig. 7a). The peak at 470 K, which is close to the boiling point of benzonitrile (463.9 K), was attributed to physically adsorbed or weakly chemisorbed benzonitrile. Therefore, only the peaks at 620 and 730 K were considered to be due to benzonitrile desorbed from acid sites and were labeled as medium strength (MS_{surf}) and strong (S_{surf}) acid sites, respectively. Since the area of the peak at 470 K increased with an increase in the Na^+ ion content, benzonitrile is weakly adsorbed on the Na^+ ion. On the other hand, the peak area due to MS_{surf} and S_{surf} acid sites decreased with an increase in the Na^+ ion content. Thus, these acid sites can be attributed to Brønsted acid sites. Modifying the acid sites with Na^+ ions, corresponding to a quarter of the protons of $H_4SiW_{12}O_{40}$, caused the peak for S_{surf} acid sites to almost disappear (Fig. 7b), indicating that S_{surf} acid sites located on the outermost surface were eliminated.

In Fig. 8, the amounts of MS_{surf} and S_{surf} acid sites are plotted against x in Na_xH_{4-}

$_x SiW_{12}O_{40}/SiO_2$. The relative amount of MS_{surf} acid sites, which was defined as $MS_{surf}/(MS_{surf} + S_{surf}) \times 100$, corresponding to the percentage of MS_{surf} acid sites, is also shown. The amount of MS_{surf} acid sites gradually decreased with an increase in the Na^+ ion content. In contrast, only a tiny amounts of S_{surf} acid sites were present on the Na-modified catalysts. The percentage of MS_{surf} acid sites for $H_4SiW_{12}O_{40}/SiO_2$ was 86% and increased with an increase in the Na^+ ion content. It is noted that almost all acid sites located on the outermost surface of $Na_3HSiW_{12}O_{40}/SiO_2$ was MS_{surf} acid sites. Thus, the amounts of MS_{surf} and S_{surf} acid sites were not consistent with any of the acid amounts (W_{bulk}, MS_{bulk}, and S_{bulk} acid sites) estimated from the NH_3-TPD profile shown in Fig. 6B.

Table 1 summarizes the heat of Ar adsorbed on $Na_xH_{4-x}SiW_{12}O_{40}/SiO_2$. Since Ar is adsorbed on the outermost surface of $Na_xH_{4-x}SiW_{12}O_{40}/SiO_2$, which is similar to benzonitrile, the heat and amount of Ar adsorbed on the catalysts correspond to the strength and amount of the acid sites located on the outermost surface, respectively. The adsorption heat of Ar was 17.9 kJ mol^{-1} for $H_4SiW_{12}O_{40}/SiO_2$ and was gradually decreased with an increase in the Na^+ ion content, indicating that the acid strength was weakened by the Na^+ ions. This was consistent with the benzonitrile-TPD result.

3.4 Modification of 15wt% $H_4SiW_{12}O_{40}/SiO_2$ with Li^+ and K^+

Fig. 9 shows isobutene conversion and selectivity for isobutene oligomerization over $Li_3HSiW_{12}O_{40}/SiO_2$, $Na_3HSiW_{12}O_{40}/SiO_2$, and $K_3HW_{12}O_{40}/SiO_2$ at 333 K for 1 h. Regardless of the kinds of alkaline metal cation, these catalysts showed high selectivity (97 – 98%) for isobutene oligomerization, although K_3HSiW/SiO_2 was slightly inactive.

4. Discussion

Acid-catalyzed reactions over solid heteropolyacids can be divided into two types [14, 16-18]: (1) surface-type catalysis, which is an ordinary heterogeneous catalytic process occurring on the surface of the solid heteropolyacids, and (2) bulk-type catalysis, also known as pseudo-liquid catalysis, in which the reactants penetrate between heteropolyanions and react in the bulk of heteropolyacid crystallites. As we have demonstrated [2], the oligomerizations of isobutene and linear butenes are surface-type catalyses over SiO_2-supported $H_4SiW_{12}O_{40}$. Thus, it is thought that the acid amount and acid strength on the outermost surface control the catalytic performance of $Na_xH_{4-x}SiW_{12}O_{40}/SiO_2$. Since $Na_4SiW_{12}O_{40}/SiO_2$ did not show any activity for the oligomerizations of isobutene and linear butenes under the present reaction conditions, it is reasonable that the reactions did not proceed on Na^+ ion but proceed only on Brønsted acid sites over the sodium-modified catalysts (x = 0, 1, 2, and 3). Since the reactions took place on the Brønsted acid sites, the oligomerizations of isobutene and linear butenes proceeded through

tertiary carbenium cations and secondary ones, respectively. However, since secondary carbenium cations are energetically unfavorable compared with tertiary carbenium cations [19], the oligomerization of linear butenes must require stronger acid sites than that of isobutene.

As shown in Fig. 2, the first-order rate constants for the isobutene oligomerization (k(*iso*-)) and linear butenes oligomerization (k(*n*-)) decreased with an increase in the Na^+ ion contents. The amounts of surface acid sites (MS_{surf} and S_{surf} acid sites) shown in Fig. 8 were also decreased with an increase in the Na^+ ion contents. However, the trends of the catalytic activity could not be explained only by those of the amounts of sole MS_{surf} or S_{surf} acid sites. For instance, although there was only a tiny amount of S_{surf} acid sites over $NaH_3SiW_{12}O_{40}/SiO_2$, the oligomerization of linear butenes over the catalyst still proceeded to some extent. On the other hand, although 64% of MS_{surf} acid sites remained on $NaH_3SiW_{12}O_{40}/SiO_2$, the catalytic activities of $NaH_3SiW_{12}O_{40}/SiO_2$ were only 40% of those of $H_4SiW_{12}O_{40}/SiO_2$. These results indicate that the oligomerizations of both isobutene and linear butenes proceeded faster on S_{surf} acid sites than on MS_{surf} ones, although the reactions proceed on both MS_{surf} and S_{surf} acid sites. Since the amount of S_{surf} acid sites was decreased more significantly than that of MS_{surf} acid sites by the modification of the catalyst with Na^+ ions, the catalytic activity for the oligomerization of linear butenes decreased more significantly than that for the oligomerization of isobutene. Thus, the selectivity for the oligomerization of isobutene was improved.

Since there was no peak assignable to S_{surf} acid sites in the benzonitrile-TPD profile for the unsupported $H_4SiW_{12}O_{40}$ [10], we think that S_{surf} acid sites located on the outermost surface formed when $H_4SiW_{12}O_{40}$ is supported on SiO_2. In other words, the interaction between the surface of SiO_2 and $H_4SiW_{12}O_{40}$ is responsible for the formation of S_{surf} acid sites. However, S_{surf} acid sites were not present on 5 wt% $H_4SiW_{12}O_{40}/SiO_2$ (data not shown), although $H_4SiW_{12}O_{40}$ is thought to be much more dispersed on SiO_2 because of the lower loading amount. Thus, we think that $H_4SiW_{12}O_{40}$, which directly interacts with the OH groups of SiO_2, does not form S_{surf} acid sites. Actually, in the separate experiments, it was demonstrated that the low loading catalysts such as 5 and 10 wt% $H_4SiW_{12}O_{40}/SiO_2$ exhibited only very low activities for the skeletal isomerization of *n*-butane to *iso*-butane (data were not shown), meaning that the acid strength of $H_4SiW_{12}O_{40}$ was rather weakened by the interaction between $H_4SiW_{12}O_{40}$ and the OH groups of SiO_2. In other words, such $H_4SiW_{12}O_{40}$ were deformed. Thus, we speculate that the second layer of $H_4SiW_{12}O_{40}$ on SiO_2 forms S_{surf} acid sites. It is reasonably considered that the strong acid sites are preferentially modified with Na^+ ions compared to the weaker acid sites. Thus, adding only a small amount of Na^+ ions eliminated S_{surf} acid sites. However, further investigation to verify this model will be needed.

5. Conclusion

In the present study, we carried out the preferential oligomerization of isobutene in an equimolar mixture of isobutene and 1-butene over Na^+-modified $H_4SiW_{12}O_{40}/SiO_2$. The selectivity for isobutene oligomerization increased with an increase in the Na^+ ion content, and that of $Na_3HSiW_{12}O_{40}/SiO_2$ was extremely high (>97%), whereas the activity decreased with an increase in the Na^+ ion content. Unmodified $H_4SiW_{12}O_{40}/SiO_2$ had both medium strength and strong acid sites on the outermost surface, which was determined by using benzonitrile-TPD. However, the strong acid sites were eliminated by the addition of Na^+ ions. $Na_3HSiW_{12}O_{40}/SiO_2$ had a negligible amount of strong acid sites, leading to a high selectivity for isobutene digomerization. $Li_3HSiW_{12}O_{40}/SiO_2$ and $K_3HSiW_{12}O_{40}/SiO_2$ also exhibited high selectivity for isobutene oligomerization.

References

[1] Japanese Patent (assigned to Idemitsu Kosan), JP 2005-015383 (2005).

[2] J. Zhang, R. Ohnishi, T. Okuhara, Y. Kamiya, Appl. Catal. A. 353 (2009) 68–73.

[3] K. Tanabe, Solid Acids and Bases, Kodansha, Tokyo, 1970, pp. 103–136.

[4] C.N. Satterfield, Heterogeneous Catalysis in Practice, McGraw-Hill Book Company, New York, 1980, pp. 151–162

[5] E. O'Donoghue and D. Barthomeuf, Zeolite 6 (1986) 267–270.

[6] T. Xu, E.J. Munson, J.F. Haw, J. Am. Chem. Soc. 116 (1994) 1962–1972.

[7] P. Cañizares and A. Carrero, Catal. Lett. 64 (2000) 239–246.

[8] T. Noda, K. Suzuki, N. Katada, M. Niwa, J. Catal. 259 (2008) 203–210.

[9] K. Suzuki, T. Noda, G. Sastre, N. Katada, M. Niwa, J. Phys. Chem. C 113 (2009) 5672–5680.

[10] Y. Kamiya, Y. Ooka, C. Obara, R. Ohnishi, T. Fujita, Y. Kurata, K. Tsuji, T. Nakajyo, T. Okuhara, J. Mol. Catal. A 262 (2007) 77–85.

[11] T. Sugii, R. Ohnishi, J. Zhang, A. Miyaji, Y. Kamiya, T. Okuhara, Catal. Today 116 (2006) 179–183.

[12] Y. Yamamoto, S. Hatanaka, K. Tsuji, K. Tsuneyama, R. Ohnishi, H. Imai, Y. Kamiya, T. Okuhara, Appl. Catal. A 344 (2008) 55–60.

[13] H. Matsuhashi, A. Furuta, Catal. Today 111 (2006) 338–342.

[14] T. Okuhara, N. Mizuno, M. Misono, Adv. Catal. 41 (1996) 113–252.

[15] M. Niwa, N. Katada, M. Sawa, Y. Murakami, J. Phys. Chem. 99 (1995) 8812.

[16] N. Mizuno, M. Misono, Chem. Rev. 98 (1998) 199–217.

[17] M. Misono, K. Sakata, Y. Yoneda, W.Y. Lee, In Proc. 7th Int. Cong. Catal., Tokyo (1980) pp 1047–1059.

[18] M. Misono, In Proc. 10th Int. Cong. Catal., Budapest (1992) pp 69–101.

[19] B.C. Gates, Catalytic Chemistry (1988) p 43.

Table 1

Heat and amount of argon adsorbed on $Na_xH_{4-x}SiW_{12}O_{40}/SiO_2$.

x in $Na_xH_{4-x}SiW_{12}O_{40}/SiO_2$	Adsorption heat of argon/kJ mol^{-1}	Adsorption amount of argon/μmol g^{-1}
0	–17.9	52
1	–17.7	29
2	–17.6	33
3	–17.4	33
4	–15.6	28

Adsorption isotherms of Ar were taken at 203–233 K. Calculations of the adsorption heat of Ar were done according to the method in Ref. [13]

Figure captions

Fig. 1 Time courses of conversions of isobutene and linear butenes during the preferential oligomerization of isobutene in a mixture of isobutene and 1-butene. Reaction conditions: temperature = 293 K, catalyst mass = 0.1 g, reactant mass = 4.8 g (mixture of 1-butene and isobutene in a 1:1 molar ratio). (●) $H_4SiW_{12}O_{40}/SiO_2$, (▲) $NaH_3SiW_{12}O_{40}/SiO_2$, (■) $Na_2H_2SiW_{12}O_{40}/SiO_2$, and (▼) $Na_3HSiW_{12}O_{40}/SiO_2$.

Fig. 2 First-order rate constants for conversions of isobutene (k(*iso*-)) and linear butenes (k(*n*-)) in the oligomerization of isobutene in a mixture of isobutene and 1-butene. (●) k(*iso*-) (△) k(*n*-), and (○) k(*iso*-)/k(*n*-) ratio.

Fig. 3 Selectivity for isobutene oligomerization as a function of conversion of isobutene. Reaction conditions: temperature = 293 K, catalyst mass = 0.1 g, reactant mass = 4.8 g (mixture of 1-butene and isobutene in a 1:1 molar ratio). (●) $H_4SiW_{12}O_{40}/SiO_2$, (▲) $NaH_3SiW_{12}O_{40}/SiO_2$, (■) $Na_2H_2SiW_{12}O_{40}/SiO_2$, and (▼) $Na_3HSiW_{12}O_{40}/SiO_2$.

Fig. 4 XRD patterns (A) and IR spectra (B) of (a) $H_4SiW_{12}O_{40}/SiO_2$, (b) $NaH_3SiW_{12}O_{40}/SiO_2$, (c) $Na_2H_2SiW_{12}O_{40}/SiO_2$, (e) $Na_3HSiW_{12}O_{40}/SiO_2$, and (f) SiO_2.

Fig. 5 NH_3-TPD profiles for (a) $H_4SiW_{12}O_{40}/SiO_2$, (b) $NaH_3SiW_{12}O_{40}/SiO_2$, (c) $Na_2H_2SiW_{12}O_{40}/SiO_2$, and (d) $Na_3HSiW_{12}O_{40}/SiO_2$.

Fig. 6 Acid amount estimated from NH_3-TPD profiles for $Na_xH_{4-x}SiW/SiO_2$. Amount of (A) total acid sites and (B) each acid sites. Broken line represents the total amount of protons calculated from the chemical formula and loading amount (15 wt%). (○) weak acid sites, (▲) medium strength acid sites, and (□) strong acid sites.

Fig. 7 Benzonitrile-TPD profiles for (a) $H_4SiW_{12}O_{40}/SiO_2$, (b) $NaH_3SiW_{12}O_{40}/SiO_2$, (c) $Na_2H_2SiW_{12}O_{40}/SiO_2$, and (d) $Na_3HSiW_{12}O_{40}/SiO_2$.

Fig. 8 Acid amount estimated from benzonitrile(BN)-TPD profiles for $Na_xH_{4-x}SiW/SiO_2$. (●) medium strength acid sites and (△) strong acid sites.

Fig. 9 Conversion of isobutene and selectivity for isobutene oligomerization as a function of conversion of isobutene. Reaction conditions: temperature = 333 K, catalyst mass = 0.1 g, reactant mass = 4.8 g (mixture of 1-butene and isobutene in a 1:1 molar ratio), and reaction time = 1 h.

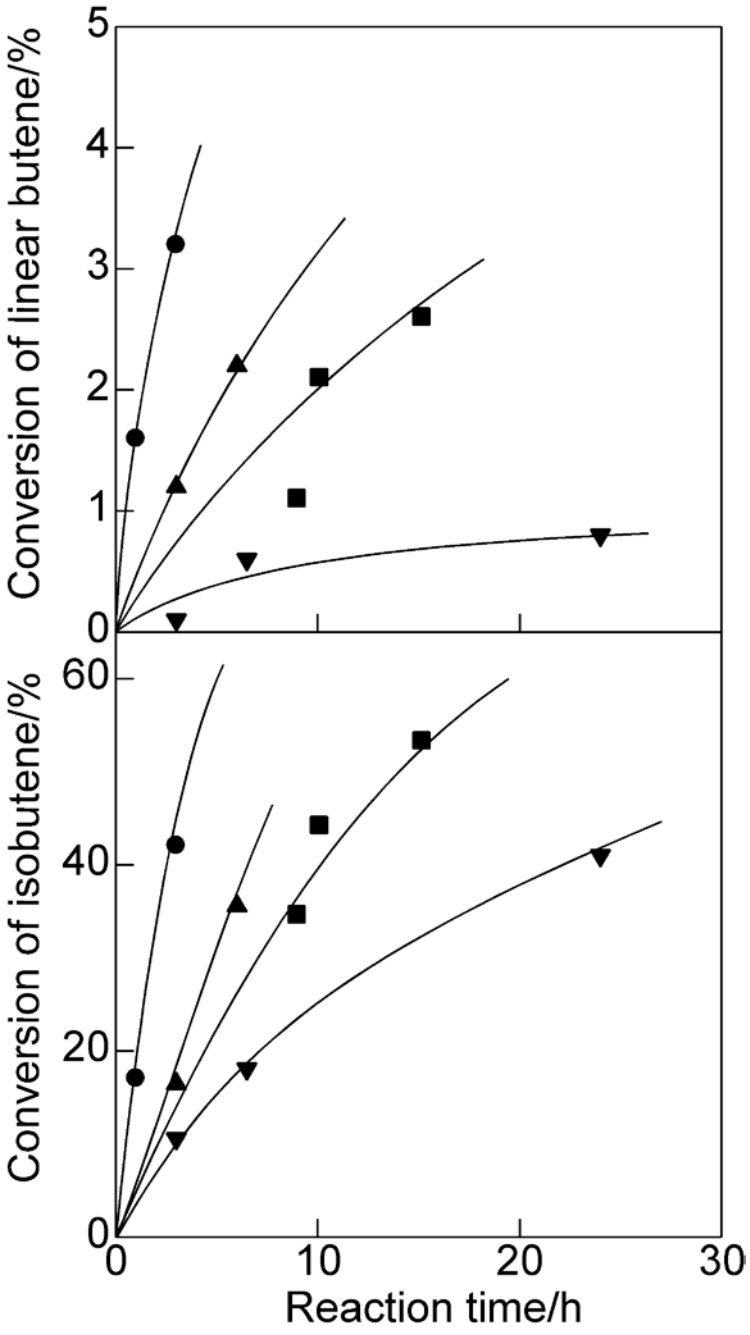

Fig. 1

Zhang et al.

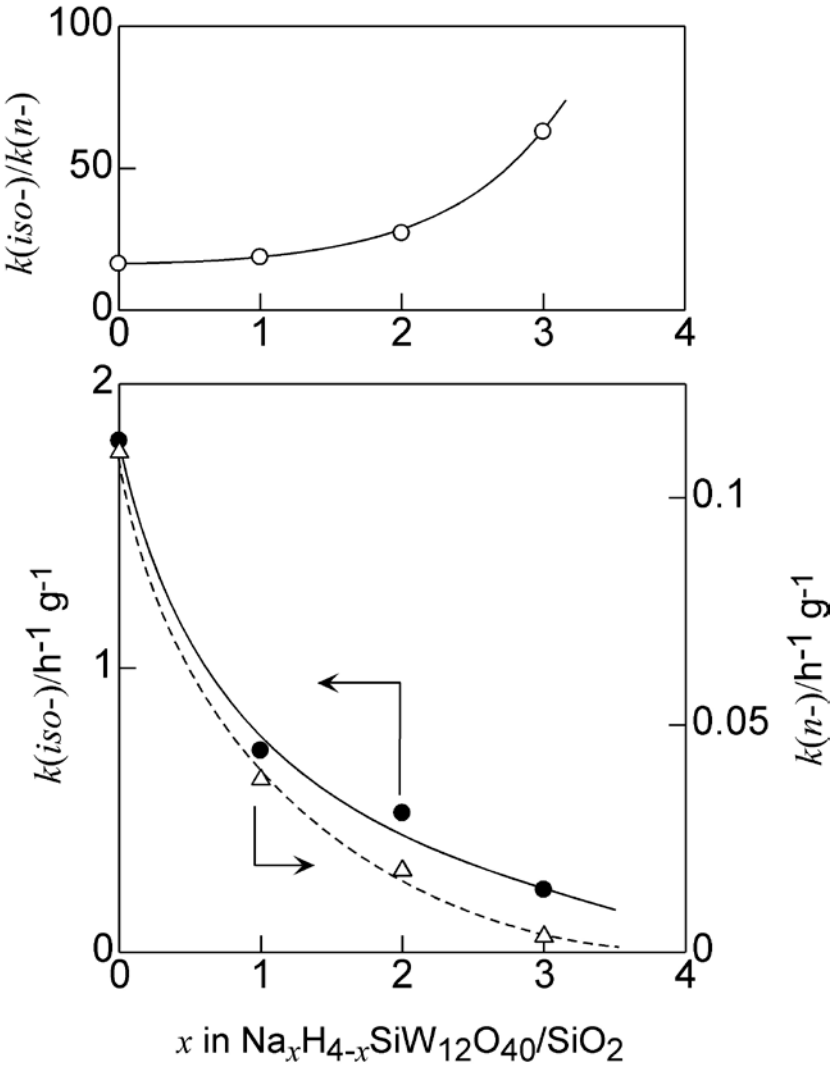

Fig. 2

Zhang et al.

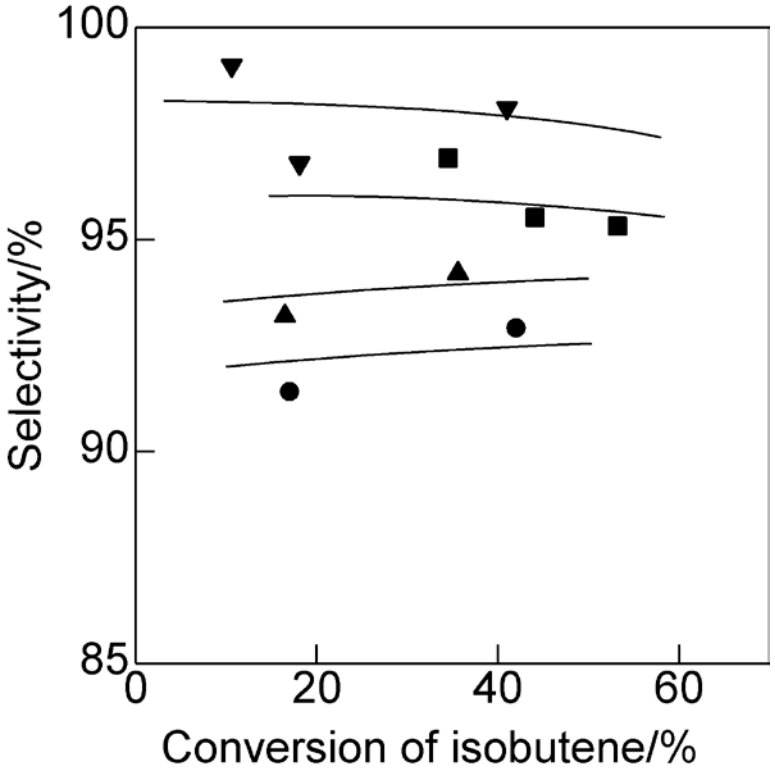

Fig. 3

Zhang et al.

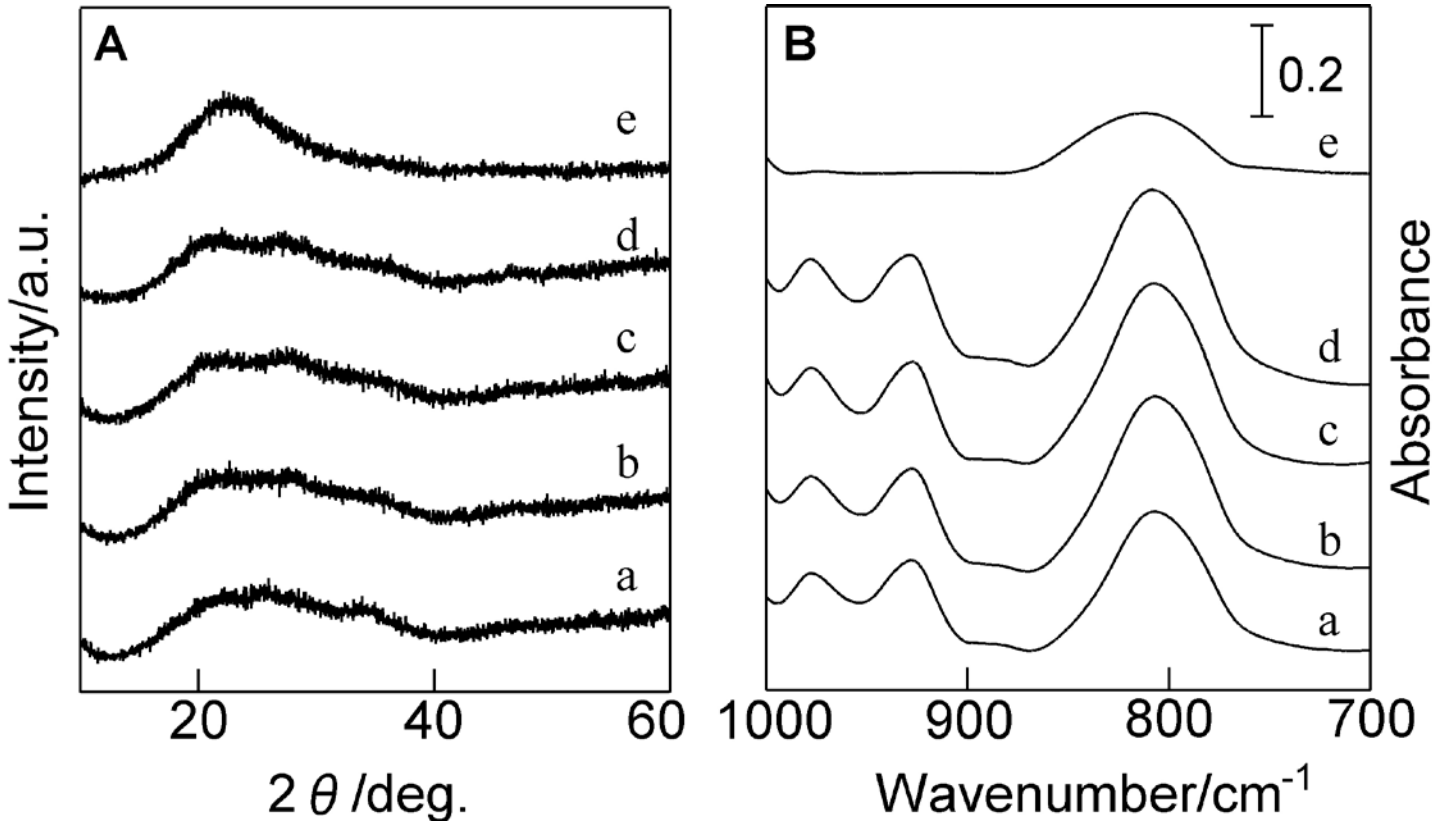

Fig. 4

Zhang et al.

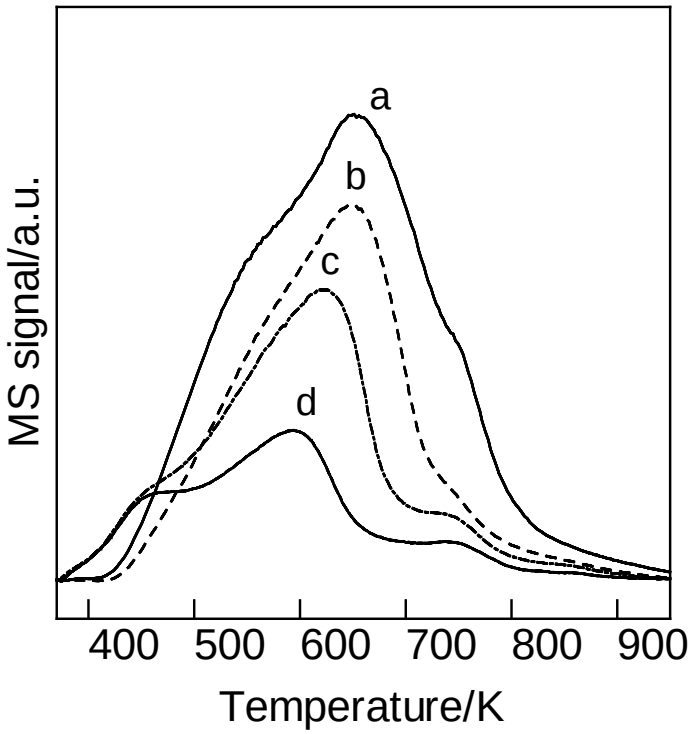

Fig. 5

Zhang et al.

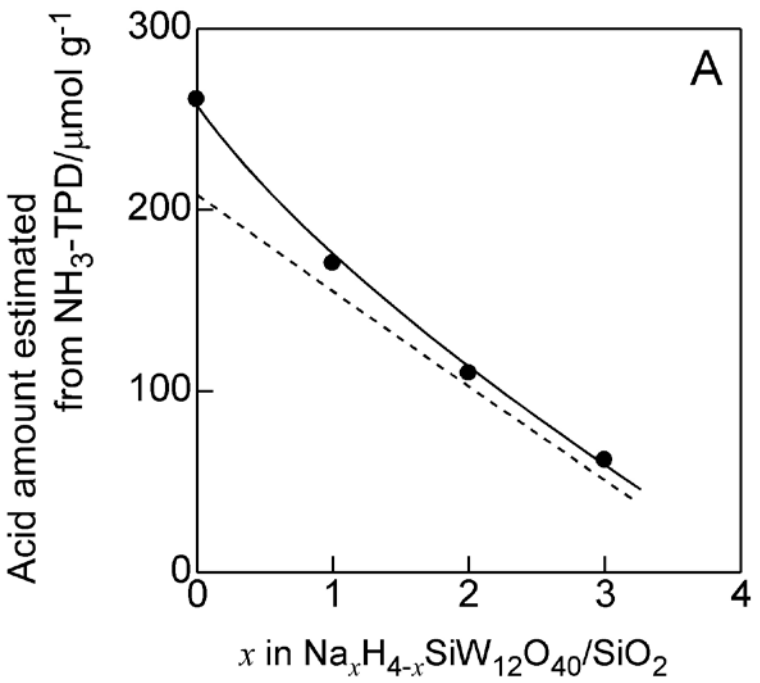

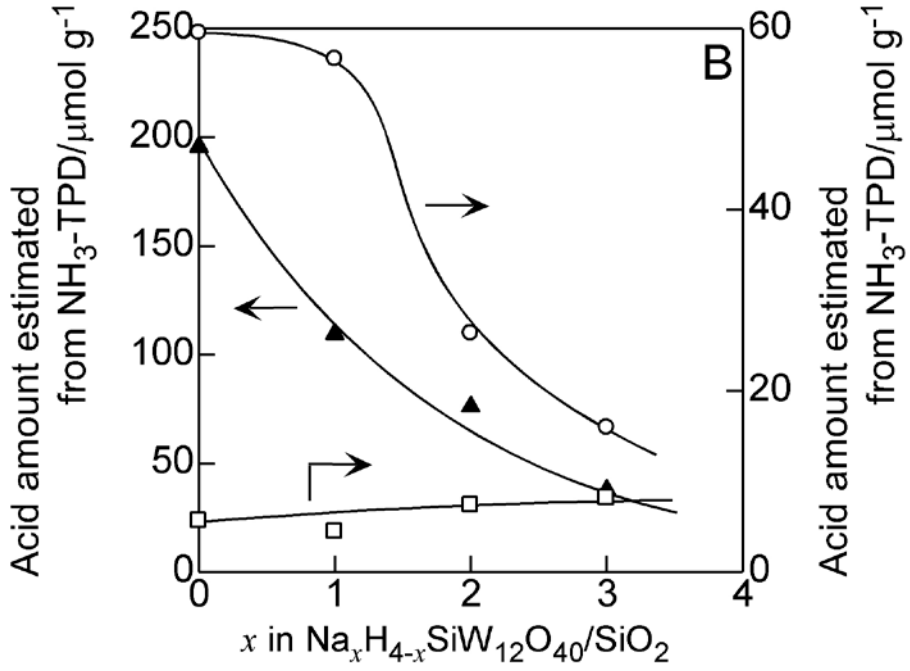

Fig. 6

Zhang et al.

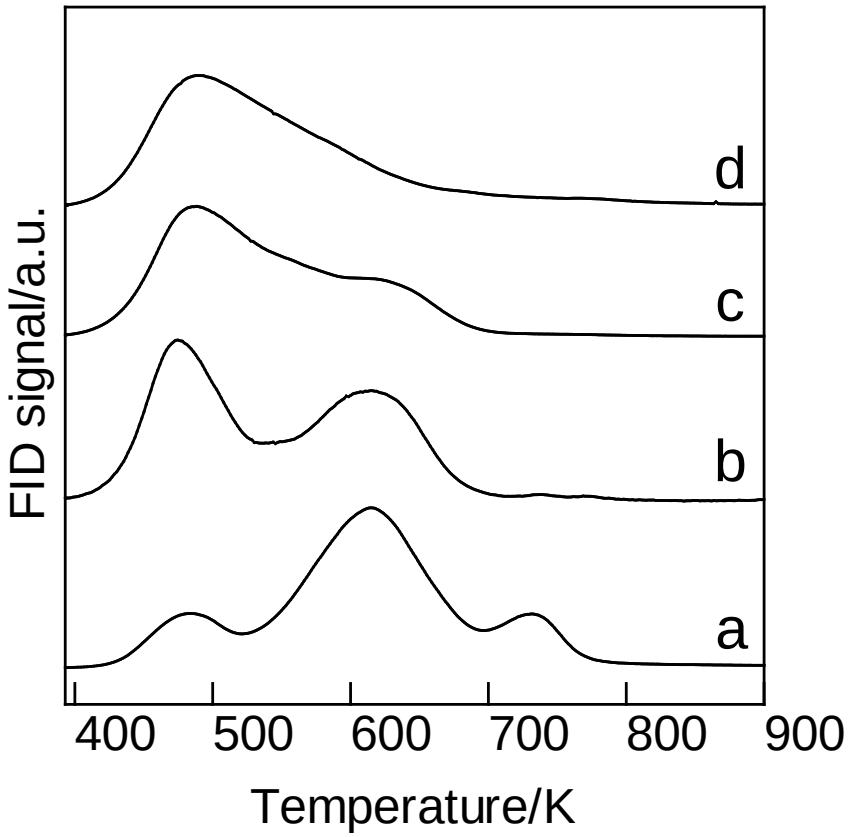

Fig. 7

Zhang et al.

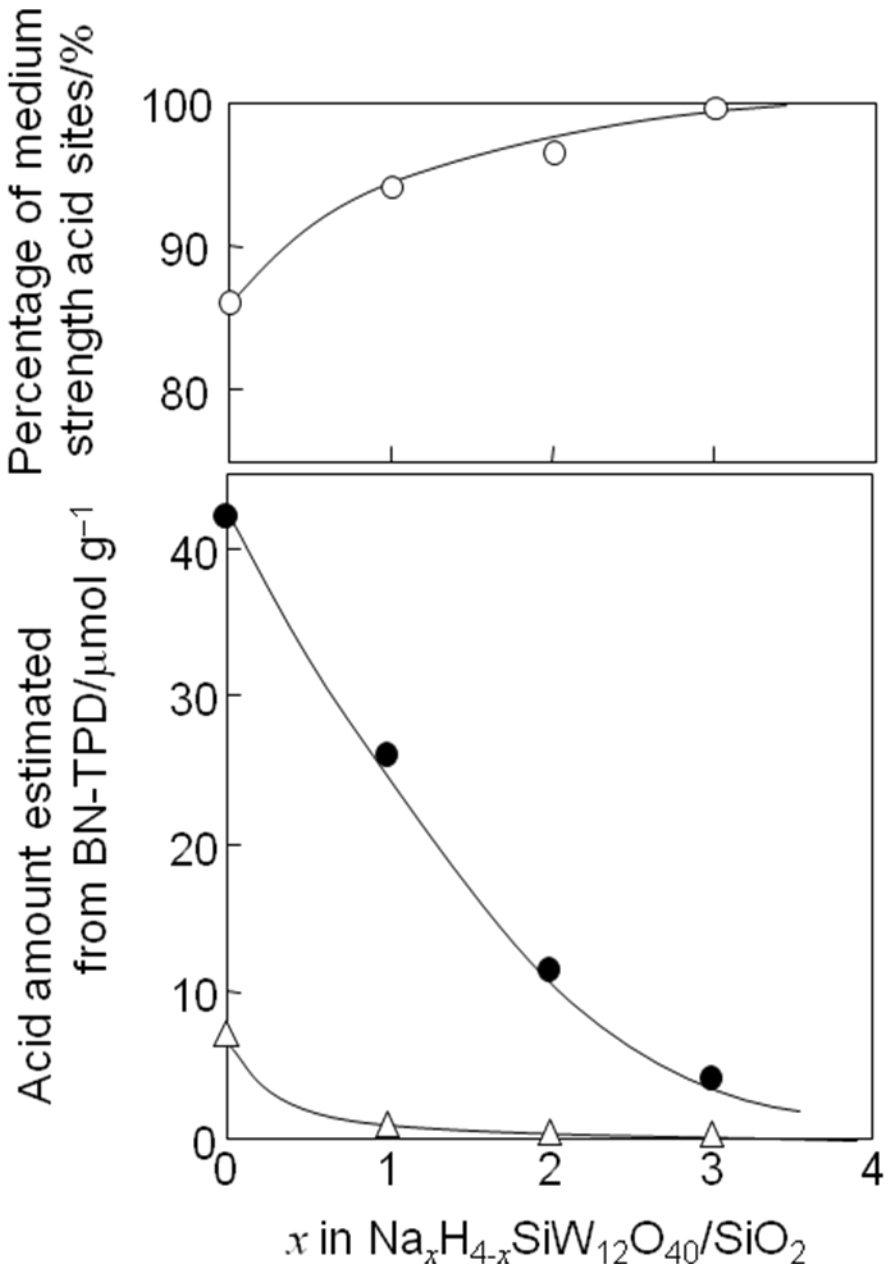

Fig. 8

Zhang et al.

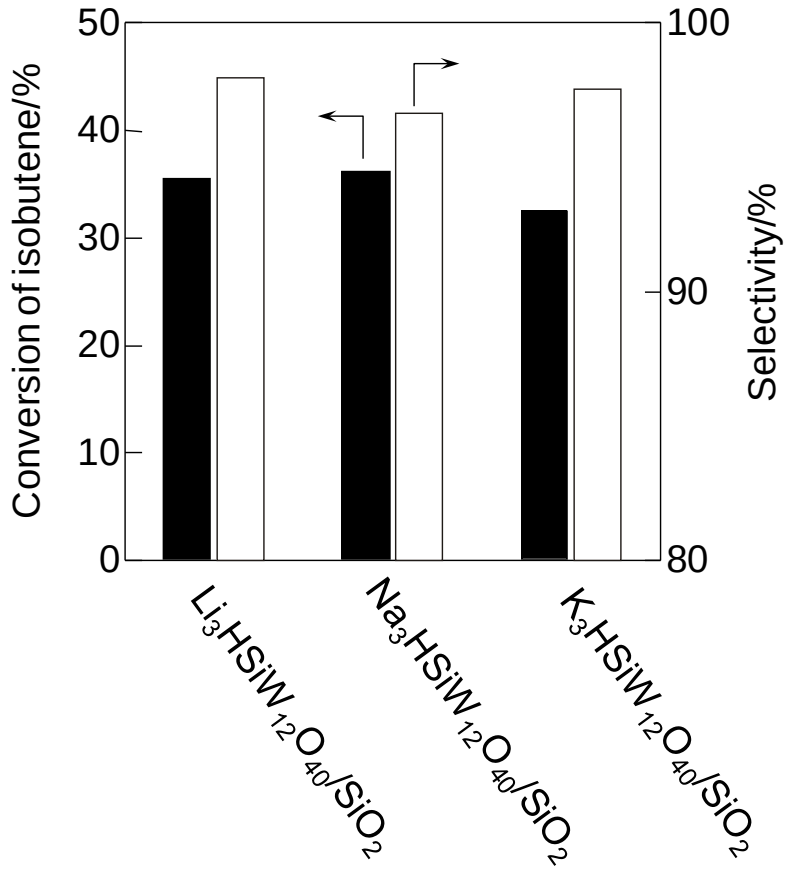

Fig. 9

Zhang et al.